Available online at www.sciencedirect.com
ScienceDirect
European Journal of Medicinal Chemistry 42 (2007) 1169–1175
EUROPEAN JOURNAL OF MEDICINAL CHEMISTRY
http://www.elsevier.com/locate/ejmech

Original article

Spectroscopic studies of DNA binding modes of cation-substituted anthrapyrazoles derived from emodin

Jia-Heng Tan [a], Yu-jing Lu [a], Zhi-Shu Huang [a], Lian-Quan Gu [a,*], Jian-Yong Wu [b,**]

[a] *School of Pharmaceutical Sciences, Sun Yat-Sen University, Guangzhou 510080, PR China*
[b] *Department of Applied Biology and Chemical Technology and State Key Lab of Chinese Medicine and Molecular Pharmacology, The Hong Kong Polytechnic University, Hung Hom, Kowloon, Hong Kong*

Received 20 November 2006; received in revised form 19 January 2007; accepted 1 February 2007
Available online 25 February 2007

Abstract

The DNA binding properties of three cation-substituted anthrapyrazole derivatives of emodin with calf thymus DNA were characterized by spectroscopic methods and the specific binding modes were elucidated. At low drug and high DNA concentrations, compound **1** with a mono-cationic amino side chain exhibited an intercalative binding mode, **2** with a much longer and more flexible di-cationic side chain exhibited an external binding mode, and **3** with a rigid di-cationic side chain exhibited both intercalative and external binding modes. The DNA binding mode of compounds was altered after structural modification. The molecular structure–DNA binding relationships found from this study may be useful for the design of anthrapyrazole derivatives with desired binding characteristics.

Keywords: Anthrapyrazole; Emodin; Amino side chain; Spectroscopic analysis; DNA binding

1. Introduction

The interaction of small molecules with DNA plays an important role in many biological processes. DNA is the molecular target of many anticancer drugs in clinical use and development. In general, most drugs have three distinct modes of non-covalent interaction with DNA, intercalative association in which a planar, aromatic moiety slides between the DNA base pairs, DNA groove binding through a combination of hydrophobic, electrostatic, and hydrogen-bonding interactions, and external binding by electrostatic attraction [1,2]. Their associative interactions with the DNA molecule can cause dramatic changes in the physiological functions of DNA [3–5]. Therefore, understanding the interactions of small molecules with DNA is of significance in the rational design of more powerful and selective anticancer agents. This can be achieved by systematically modifying the structural features of the lead compound, and analyzing the subsequent changes in the DNA binding properties [6–8].

Anthrapyrazoles (APs), or anthraquinones bearing a pyrazole ring, represent a class of potential anticancer drugs, some of which have demonstrated clinical efficacy for the treatment of breast cancer [9,10]. We have recently synthesized a series of new anthrapyrazole derivatives from emodin with various cationic alkyl amino side chains attached to the pyrazole ring [11]. These emodin-derived anthrapyrazoles showed much stronger binding affinity to calf thymus DNA and cytotoxicity against several tumor cell lines than emodin. This study was to characterize the specific DNA binding modes of these anthropyrazoles so as to gain better understanding of their interactions with the DNA molecule and their cytotoxic activities.

* Corresponding author. Tel./fax: +86 20 84110272.
** Corresponding author. Tel.: +852 3400 8671; fax: +852 2364 9932.
E-mail addresses: cedc42@zsu.edu.cn (L.-Q. Gu), bcjywu@polyu.edu.hk (J.-Y. Wu).

0223-5234/$ - see front matter © 2007 Elsevier Masson SAS. All rights reserved.
doi:10.1016/j.ejmech.2007.02.002

2. Experimental

2.1. Materials

Three cation-substituted anthrapyrazole derivatives **1**–**3** (Fig. 1) were chosen for the DNA binding mode studies, which were prepared as described previously [11] (**1**, **2** and **3** here correspond to **7**, **10** and **13** in previous study, respectively). All chemicals were of analytical grade, and used without further purification. The sodium phosphate buffer (pH 6.3, 10 mM NaH_2PO_4–Na_2HPO_4, 100 mM NaCl) used in all experiments was prepared with double distilled deionized water. The calf thymus (CT) DNA (Sigma, St Louis, MO) was dissolved in double distilled deionized water with 50 mM NaCl, and dialyzed against a buffer solution for 2 days. The DNA concentration was determined by absorption spectrometry at 260 nm using a molar extinction coefficient 6600 $M^{-1}\,cm^{-1}$. The ratio $A_{260}/A_{280} > 1.80$ was used as an indication of a protein-free DNA. The DNA solution was stored for a short period of time at 4 °C if not used immediately [12].

2.2. Methods

The following spectrometric measurements were all performed at 20 °C in a quartz cuvette of 1 cm path length, and the sample solution was stirred for 5 min before hand.

2.2.1. Absorption titration and ligand self-association measurement

Absorption titration was performed at a fixed drug concentration (20 μM) with various concentrations (0–135 μM) of CT DNA. The absorption spectra were recorded on a Shimadzu UV-2501 spectrophotometer. The absorption parameters, including red shift, hypochromicity and isosbestic point were found from the absorption spectra. For the ligand self-association measurement, selected volumes of a concentrated drug solution were added into the sodium phosphate buffer to generate a range of concentrations from 1 to 225 μM. The parameters derived from the absorption spectra were used to calculate the apparent molar extinction coefficients.

2.2.2. Ethidium bromide displacement measurement

Small aliquots of a concentrated drug solution were added into a solution of CT DNA (2 μM) and ethidium bromide (EB, 2.5 μM) at various final concentrations (0–54 μM). The corresponding fluorescence spectra were recorded at Ex 546 nm and Ex/Em 10 nm/10 nm on a Shimadzu RF-5301PC fluorescence spectrophotometer. The drug concentration required to reduce the relative fluorescence by 50% was derived from the plot of relative fluorescence at Em 595 nm versus drug dose.

2.2.3. Circular dichroism titration

Circular dichroism (CD) spectra were recorded on a Jasco J-810 spectropolarimeter and with the JASCO software. CD titration was first performed at a fixed CT DNA concentration (200 μM) with various concentrations (0–66 μM) of the drugs using the instrument parameters of 220–650 nm wavelength, 1 nm bandwidth, 100 millidegree sensitivity, and 1 s response time, with an average of four scans. Then, the induced CD (ICD) spectra were recorded at 200 μM drug and 1000 μM DNA in the range of 350–550 nm at 1 nm bandwidth, 5 millidegree sensitivity, and 4 s response time with an average of eight scans.

3. Results and discussion

3.1. DNA binding properties based on absorption titration

Fig. 2 shows the absorption spectra of compounds (20 μM) at 0–135 μM CT DNA concentrations; Table 1 summarizes the corresponding absorption parameters. Both **1** and **3** bound with CT DNA exhibited marked hypochromicity and red shifts, with the maxima at 457 nm for **1** (22%, 10 nm), and at 463 nm for **3** (21%, 7 nm). Clear isosbestic points were also observed in both the spectra at 487 nm for **1** and at 499 nm for **3**. The overall spectral changes with hypochromicity, red shift and isosbestic point induced by binding planar polyaromatic drugs to DNA are suggestive of intercalative association as a major binding mode [13,14]. The designation of intercalative binding mode to these two compounds will be further discussed below.

In contrast, the absorption spectra of **2** at various DNA concentrations exhibited moderate hypochromicity (16%) but insignificant red shift (3 nm) and no clear isosbestic point. This compound may assume a different DNA binding mode from that of the other two. The hypochromicity in the absorption spectra is mostly attributed to the interaction between the electronic states of the compound chromophore and those of the DNA bases [13]. On the other hand, the red shift is

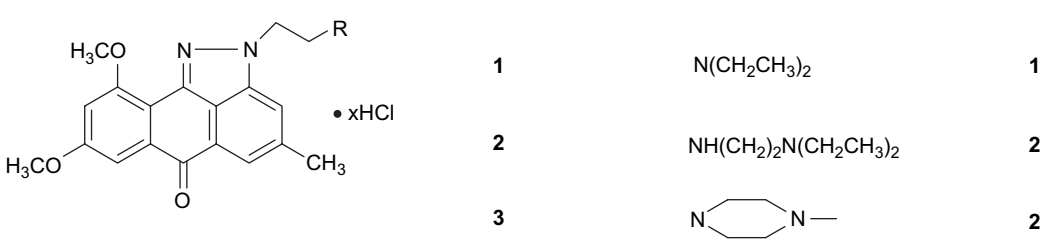

Fig. 1. Molecular structures of anthrapyrazole derivatives from emodin.

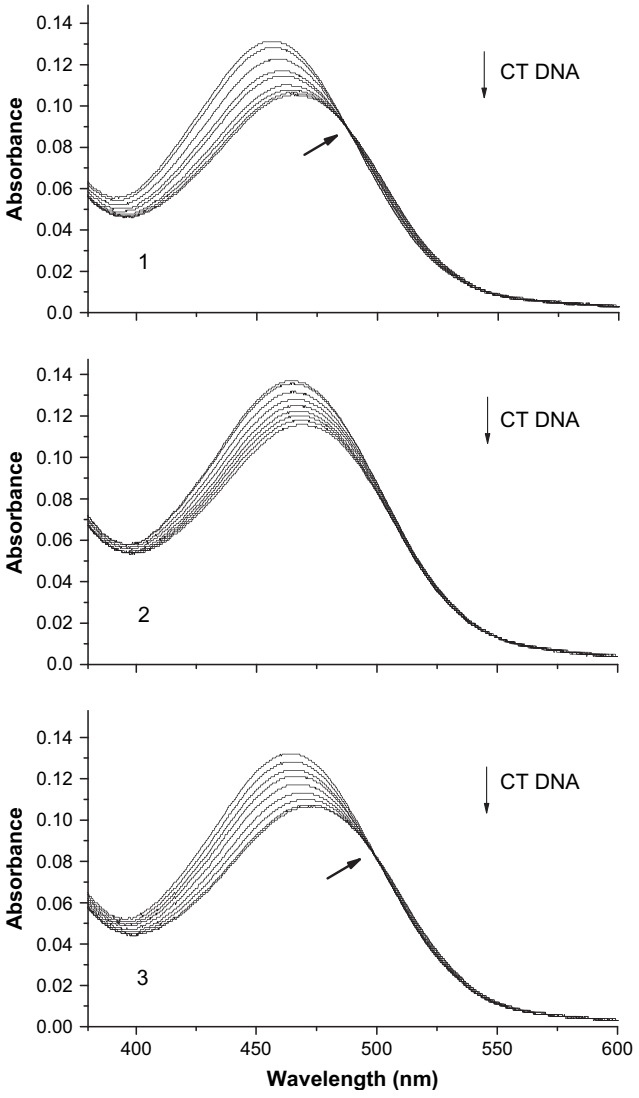

Fig. 2. Absorption titration of **1**–**3** (20 μM) at increasing CT DNA concentration (arrow: 0–165 μM).

associated with a decrease in the energy gap between the highest and the lowest occupied molecular orbitals (HOMO and LUMO) when the drug compound binds to DNA [15,16]. The lack of hypochromicity and red shift in **2** revealed its distinct chromophore environment in the drug–DNA complex compared to **1** and **3**. Moreover, clear isosbestic points in **1** and **3** indicate that there are at least two spectroscopically distinct chromophores (free and bound) in the solution [8,17,18]. The lack of an isosbestic point in **2** may suggest that its chromophore environment was not altered after the interaction with DNA. In other words, intercalation may be ruled out as a major binding mode of **2** with the DNA.

Table 1
Photometric properties of **1**–**3** in contact with CT DNA

Compound	λ_{max} (nm)	Red shift (nm)	Hypochromicity (%)	Isosbestic point (nm)	C_{50} (μM)
1	457	10	22	487	12
2	466	3	16	None	21
3	463	7	21	499	14

3.2. Ethidium bromide displacement characteristics

Fig. 3 shows the relative fluorescence intensity (FI; I/I_0) of EB versus the concentration of **1**–**3**. The C_{50} values (concentration of the compound that causes a 50% reduction in the fluorescence of the calf thymus DNA–Ethidium bromide complex) are summarized in Table 1. The results show that the displacement of EB by **1** and **3** was much more effective than **2**. Ethidium bromide (EB) is a classical DNA intercalative agent which emits intense fluorescence after binding to the DNA. The fluorescence quenched by a compound added to the EB–DNA mixture solution is proportional to the amount of EB replaced by the compound which binds to the DNA in different binding modes [19–22]. Anthrapyrazole derivatives **1**–**3** possessed the same chromophore but different amino side chains as the regulative element. Therefore, the more effective EB displacement by **1** and **3** may be associated with their intercalative DNA binding mode, and the less effective EB displacement by **2** may be due to its lack of this binding mode, as proposed in last section.

3.3. Circular dichroism characteristics

Fig. 4a shows the CD spectra at a fixed CT DNA concentration (200 μM) and with increasing concentration of **1**–**3** from 0 to 66 μM ([DNA]/[drug] > 3 for all). In the absence of a drug, the CD spectrum of CT DNA was of the typical B-form, with a positive Cotton effect near 277 nm due to base stacking and a negative Cotton effect near 245 nm due to polynucleotide helicity [23,24]. The ellipticity intensity of compounds **1**–**3** at 245 nm (Fig. 4b) decreased but that at 277 nm (Fig. 4c) increased with the increase in the drug concentration. The similar declining trend of ellipticity intensity

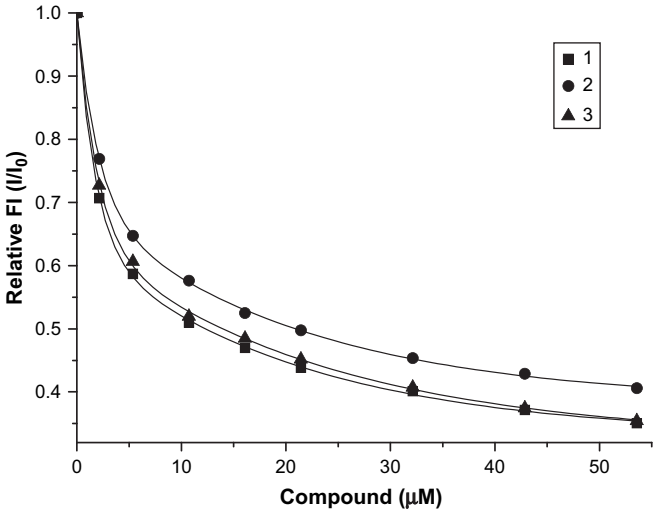

Fig. 3. Relative fluorescence intensity decrease of EB (2.5 μM) induced by the competitive binding of **1**–**3** (0–54 μM) to CT DNA (2.0 μM).

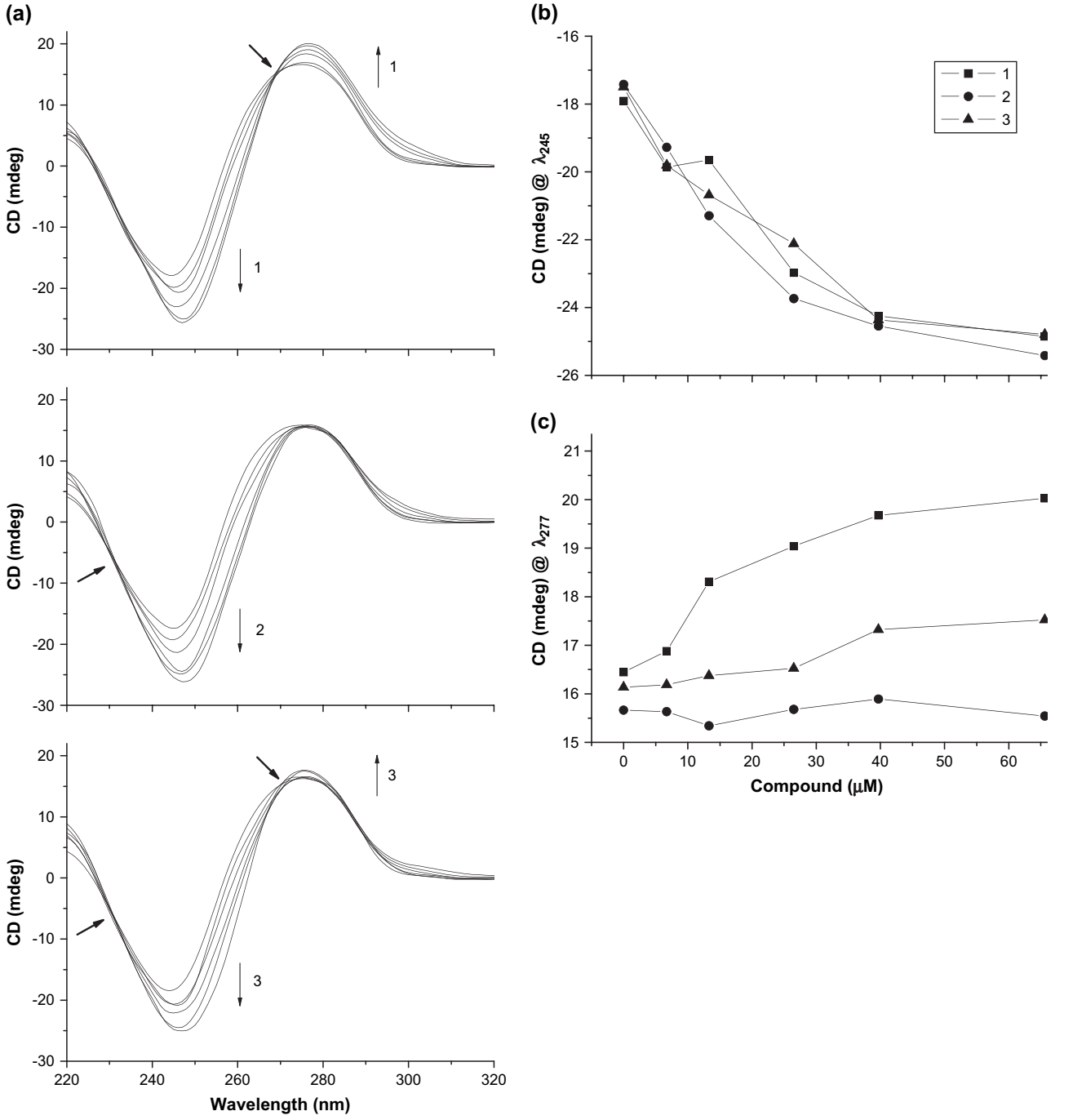

Fig. 4. CD titration spectra of CT DNA (200 μM) at increasing drug concentration (arrow: 0–66 μM; [DNA]/[drug] > 3) (a), and the corresponding ellipticity intensities at 245 nm (b), and 277 nm (c).

versus concentration at 245 nm with all three compounds is suggestive of their similar ability in inducing helix helicity. On the other hand, the ellipticity intensity at 277 nm increased much more significantly with the progressive addition of **1** than with **2** and **3**, which is suggestive of a much stronger intercalative binding of **1** to the DNA than the other two compounds. Furthermore, the dramatic ellipticity intensity increase with **1** at 277 nm may be associated with a reduced DNA winding angle as previous studies have shown an inverse correlation of the intensity at 277 nm with the DNA winding angle [25,26]. This is in accordance with the intercalative binding mode that the winding angle is reduced by the ligand chromophore inserted into two adjacent base pairs of the DNA [14,27]. On the other hand, the addition of **2** resulted in little increase in the ellipticity intensity at 277 nm, which is again consistent with its lack of intercalative interaction with the DNA as observed in the above two sections. Furthermore, **3** caused a slight and gradual increase in the ellipticity intensity at 277 nm with a moderate red shift, suggesting that **3** had a mixed effect of **1** and **2** on the DNA conformation.

The presence of a clear isoelliptic point at 269 nm for **1** and at 231 nm for **2** in the CD spectra suggests that **1** and **2** formed two different drug–DNA complexes with different binding geometry [28]. On the other hand, the presence of two isoelliptic points at 271 nm and 231 nm in the CD titration spectra of **3** suggests that **3** had a mixed binding mode of **1** and **2**.

3.4. ICD characteristics

Further evidence for the binding modes of **1**–**3** was attained from the induced CD spectra in the range of 350–550 nm corresponding to the anthrapyrazole chromophore (Fig. 5). Although these compounds are achiral molecules, they displayed the ICD signal after forming complexes with the DNA whose characteristics were dependent on the position and the orientation with respect to the polynucleotide bases. The compound **1**–CT DNA complex exhibited a relatively strong positive ICD band. The positive ICD spectrum in this region is characteristic of the intercalated chromophore with the anthrapyrazole moiety aligning perpendicularly to the long axis of the DNA base pairs [16,29]. The compound **2**–CT DNA complex exhibited a weaker and biphasic ICD signal. The biphasic shape of the CD spectrum, i.e. a negative band at lower wavelengths and a positive band at higher wavelengths, is characteristic of chromophores with a right-hand orientation [30]. The exciton CD observed in the drug absorption region is generally viewed as a case of groove binding or external stacking with the formation of ligand dimers (or higher order complexes) in the drug–DNA complexes [31,32]. However, the groove binding mode should be ruled out for **2** based on the following considerations. First of all, the Induced CD by groove binding usually has a positive signal and is much stronger than those induced by other binding modes. Secondly, in the above absorption and CD titration we have proved that **2** mixed with CT DNA still had a relatively free chromophore not interfering with the DNA helix. This situation is more consistent with an external binding mode. Thirdly, **2** may be too bulky and positively charged to lie in the grooves of DNA. Moreover, **2** does not have the structural features of the groove binders reported previously [7]. As a dimeric molecule, **2** has four cationic centers with long and flexible side chains which obstruct the chromophore from accessing the DNA base pairs but favor external binding through electrostatic attraction. The **3**–CT DNA complex exhibited an ICD signal level between that of **1** and **2** and a zero ICD signal in the range of 430–445 nm, which suggests a mixed binding mode for **3**.

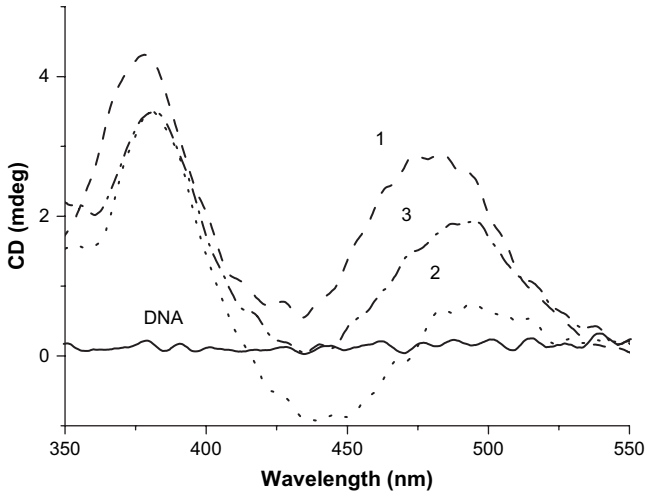

Fig. 5. ICD spectra of **1**–**3** (200 μM) in contact with CT DNA (1000 μM).

3.5. Ligand self-association ability

Ligand self-association, the formation of dimers or higher-order polymeric structures often occurs with planar aromatic drugs including anthrapyrazoles at high ligand concentrations [33,34]. To examine the dimer-forming abilities of **1**–**3** relevant to their DNA binding modes found in the ICD characteristics, we measured the molar extinction coefficient ε_{app} of the compounds at their λ_{max} at various concentrations (Fig. 6). The coefficient ε_{app} of **1** increased gradually from a low drug concentration to a maximum and then decreased gradually with further increase in the concentration; the coefficients of **2** and **3** increased more sharply to a peak with the drug concentration from a very low level and then dropped rapidly. According to previous studies [35,36], the low ε_{app} values of **1**–**3** at 1 μM, approximately 5000, are suggestive of the compounds existing as monomeric species, and the gradual decrease of their ε_{app} values at 30 μM or higher is suggestive of homologous dimers. In the concentration range from 1 μM to 30 μM, the compounds are in the transition region from monomer to dimer form. The different trends of ε_{app} versus the drug concentration with the compounds in this region are indicative of their different manners of ligand self-association. It is generally believed that the decreasing ε_{app} at increasing drug concentration is the characteristic of the dimer species [33,35]. According to this hypothesis, **2** and **3** started to form dimers at a concentration of about 2 μM which is much lower than that of **1** (30 μM).

The results here show a higher degree of ligand self-association in the di-cationic compounds **2** and **3** than in **1**. In

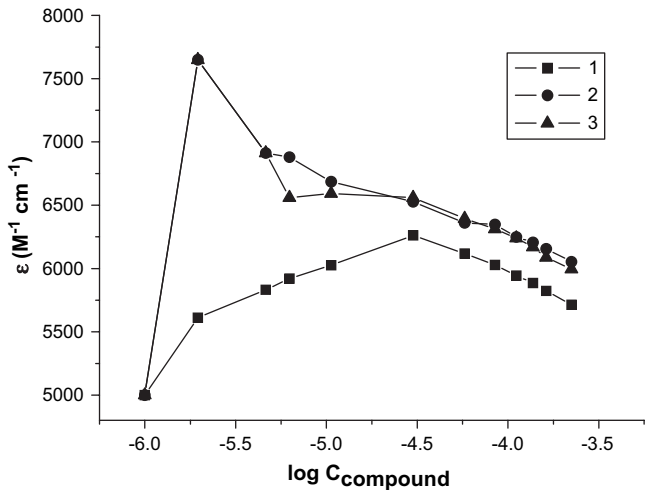

Fig. 6. Concentration dependence of the molar extinction coefficients with free **1**–**3** (1 μM–225 μM) at their respective λ_{max} (457 nm for **1**, 466 nm for **2** and 463 nm for **3** as shown in Table 1).

compound **1**, the dimeric nature can be quenched when it is intercalated into the DNA macromolecule. In compound **2**, however, its long and flexible cationic side chains are favorable for external binding, as discussed in last section. With the ligand self-association ability, the drug molecules may bind on the surface of DNA, can attract other drug molecules in the solution and, subsequently, assemble into dimers or higher orders of complexes on the DNA surface. Moreover, as a dimer, compound **2** possess more cationic centers which help to stabilize the drug–DNA complex. These two features of compound **2** also favor the external binding with outside stacking. Compound **3** also has similar features. Therefore, compounds **2** and **3** may facilitate the external binding with outside stacking due to their structural features and stronger ligand self-association ability.

3.6. DNA binding mode and cytotoxicity

Drugs can interact with DNA through intercalative association and binding locations, which may cause conformational changes in the regular helical structure, unwinding the DNA at the binding site and interfering with the function of DNA binding enzymes such as DNA topoisomerases and DNA polymerases [4]. The inhibition of topoisomerase II has been recognized as a general mechanism of action for the antitumor and cytotoxic effects of DNA intercalators [6]. In our previous study [11], compound **1** exhibited the most potent cytotoxicity against three different tumor cell lines with the lowest IC_{50} values among the three compounds examined in this study (Table 2). Since compounds **1** and **3** had the similar DNA binding affinity according to their similar K_i values, the stronger cytotoxicity of **1** may be partially attributed to its stronger intercalative DNA binding property than **3**. On the other hand, the generally lower cytotoxicity of compound **2** than both **1** and **3** may be partially attributed to its external binding with outside stacking and lack of ability in stabilizing the DNA–intercalator–topoisomerase ternary complex. Therefore, strong intercalative binding with DNA may be an important consideration in the design and synthesis of cation-substituted anthrapyrazoles for anticancer agents.

4. Conclusion

The DNA binding modes of three cation-substituted anthrapyrazoles derived from emodin have been elucidated based on spectroscopic studies. The different binding modes of the compounds may be attributed to their difference in the side chain flexibility and charge density. Compound **1** with a mono-cationic side chain was assigned intercalative binding mode; compound **2** with a long and flexible side chain and two adjacent cationic centers was assigned external binding mode; compound **3** with a rigid di-cationic side chain appeared to have multiple binding modes including intercalative as major and external binding as minor mode according to its intermediate spectral features between **1** and **2**. The molecular structure–DNA binding relationships found from this study will be useful for designing anthrapyrazole derivatives with desired binding characteristics.

Table 2
Binding constants (K_i) of emodin and compounds **1**–**3** with CT DNA and their IC_{50} cytotoxicity values (μM) against three tumor cell lines (B16 – mouse melanoma, HepG2 – human hepatocellular carcinoma, LLC – Lewis lung carcinoma) [11]

Compound	K_i ($\times 10^{-5}$ M^{-1})	B16	HepG2	LLC
Emodin	0.68	>100	55.1	>100
1	5.52	3.6	4.9	4.5
2	2.53	10.1	37.6	12.8
3	6.98	20.1	7.2	8.9

Acknowledgements

This work was supported financially by the National Natural Science Foundation of China (20472117), the Science Foundation of Zhuhai (PC20041131), and the Hong Kong Polytechnic University through the State Key Lab of Chinese Medicine and Molecular Pharmacology in Shenzhen.

References

[1] Y. Cao, X.-W. He, Spectrochim. Acta A, Mol. Biomol. Spectrosc. 54A (1998) 883–892.
[2] B. Hwa Yun, S. Hee Jeon, T.-S. Cho, S. Yoon Yi, U. Sehlstedt, S.K. Kim, Biophys. Chem. 70 (1998) 1–10.
[3] P.B. Dervan, Bioorg. Med. Chem. 9 (2001) 2215–2235.
[4] L.H. Hurley, Nat. Rev. Cancer 2 (2002) 188–200.
[5] B. Gold, Biopolymers 65 (2002) 173–179.
[6] M.F. Brana, M. Cacho, A. Gradillas, B. De Pascual-Teresa, A. Ramos, Curr. Pharm. Des. 7 (2001) 1745–1780.
[7] S. Neidle, Nat. Prod. Rep. 18 (2001) 291–309.
[8] W.B. Tan, A. Bhambhani, M.R. Duff, A. Rodger, C.V. Kumar, Photochem. Photobiol. 82 (2006) 20–30.
[9] H.D. Showalter, J.L. Johnson, J.M. Hoftiezer, W.R. Turner, L.M. Werbel, W.R. Leopold, J.L. Shillis, R.C. Jackson, E.F. Elslager, J. Med. Chem. 30 (1987) 121–131.
[10] C. Sissi, S. Moro, S. Richter, B. Gatto, E. Menta, S. Spinelli, A.P. Krapcho, F. Zunino, M. Palumbo, Biochem. Pharmacol. 59 (2001) 96–103.
[11] J.-H. Tan, Q.-X. Zhang, Z.-S. Huang, Y. Chen, X.-D. Wang, L.-Q. Gu, J.Y. Wu, Eur. J. Med. Chem. 41 (2006) 1041–1047.
[12] W. Zhong, J.-S. Yu, W. Huang, K. Ni, Y. Liang, Biopolymers 62 (2001) 315–323.
[13] H.M. Berman, P.R. Young, Annu. Rev. Biophys. Bioeng. 10 (1981) 87–114.
[14] E.C. Long, J.K. Barton, Acc. Chem. Res. 23 (1990) 271–273.
[15] C.V. Kumar, E.H.A. Punzalan, W.B. Tan, Tetrahedron 56 (2000) 7027–7040.
[16] N.K. Modukuru, K.J. Snow, B.S. Perrin, A. Bhambhani, M. Duff, C.V. Kumar, J. Photochem. Photobiol. A, Chem. 177 (2006) 43–54.
[17] J.E. Rogers, S.J. Weiss, L.A. Kelly, J. Am. Chem. Soc. 122 (2000) 427–436.
[18] M.R. Bugs, M.L. Cornelio, Eur. Biophys. J. 31 (2002) 232–240.
[19] B.C. Baguley, W.A. Denny, G.J. Atwell, B.F. Cain, J. Med. Chem. 24 (1981) 170–177.
[20] D.L. Boger, B.E. Fink, S.R. Brunette, W.C. Tse, M.P. Hedrick, J. Am. Chem. Soc. 123 (2001) 5878–5891.
[21] M. Labieniec, T. Gabryelak, J. Photochem. Photobiol. B, Biol. 82 (2006) 72–78.
[22] T. Jia, Z.-X. Jiang, K. Wang, Z.-Y. Li, Biophys. Chem. 119 (2006) 295–302.

[23] Z. Wang, D. Liu, S. Dong, Biophys. Chem. 87 (2000) 179–184.
[24] V. Uma, M. Kanthimathi, T. Weyhermuller, B.U. Nair, J. Inorg. Biochem. 99 (2005) 2299–2307.
[25] A. Chan, R. Kilkuskie, S. Hanlon, Biochemistry 18 (1979) 84–91.
[26] B.B. Johnson, K.S. Dahl, I. Tinoco Jr., V.I. Ivanov, V.B. Zhurkin, Biochemistry 20 (1981) 73–78.
[27] J.M. Benevides, G.J. Thomas Jr., Biochemistry 44 (2005) 2993–2999.
[28] F.-M. Chen, F. Sha, Biochemistry 37 (1998) 11143–11151.
[29] M. Eriksson, B. Norden, Meth. Enzymol. 340 (2001) 68–98.
[30] K.M. Sovenyhazy, J.A. Bordelon, J.T. Petty, Nucleic Acids Res. 31 (2003) 2561–2569.
[31] N.E. Mukundan, G. Petho, D.W. Dixon, M.S. Kim, L.G. Marzilli, Inorg. chem. 33 (1994) 4676–4687.
[32] B. Norden, T. Kurucsev, J. Mol. Recognit. 7 (1994) 141–155.
[33] G. Schwarz, S. Klose, W. Balthasar, Eur. J. Biochem. 12 (1970) 454–460.
[34] J.A. Hartley, K. Reszka, E.T. Zuo, W.D. Wilson, A.R. Morgan, J.W. Lown, Mol. Pharmacol. 33 (1988) 265–271.
[35] J.B. Chaires, N. Dattagupta, D.M. Crothers, Biochemistry 21 (1982) 3927–3932.
[36] I. Haq, J.E. Ladbury, B.Z. Chowdhry, T.C. Jenkins, J. Am. Chem. Soc. 118 (1996) 10693–10701.